Two-color vector-soliton interactions in nematic liquid crystals in the local response regime

Two-color vector-soliton interactions in nematic liquid crystals in the local response regime

Benjamin D. Skuse* and Noel F. Smyth†

School of Mathematics and Maxwell Institute for Mathematical Sciences, The King's Buildings, University of Edinburgh, Edinburgh, Scotland EH9 3JZ, United Kingdom

(Received 27 September 2007; published 18 January 2008)

The propagation and interaction of two bulk solitary waves, termed nematicons, in a nematic liquid crystal are studied in the local limit. These two nematicons are based on light of two different wavelengths, and so are referred to as two color nematicons. Under suitable boundary conditions the two nematicon beams of different wavelengths can couple, creating a self-localized vector solitary wave. Due to the different diffraction coefficients and indices of refraction for each wavelength, the vector solitary wave shows walk-off. Using a suitable trial function in an averaged Lagrangian formulation of the two color nematicon equations, approximate equations governing the evolution of the two color nematicons are derived. These approximate equations are extended to include the diffractive radiation shed as the nematicons evolve. Excellent agreement is found for the walk-off as given by these approximate equations and by full numerical solutions of the nematicon equations. It is shown that the inclusion of the effect of the shed diffractive radiation is vital in order to obtain this excellent agreement.

DOI: 10.1103/PhysRevA.77.013817 PACS number(s): 42.65.Tg, 42.70.Df

I. INTRODUCTION

The study of the propagation of guiding, self-supporting, coherent, two dimensional nonlinear beams (spatial solitary waves) in nematic liquid crystals has become an active area of experimental and theoretical research within the last few years. The experimental existence of these nonlinear beams was first demonstrated by Assanto and co-workers [1–4], who named them nematicons. 2+1 dimensional solitary wave solutions of the nonlinear Schrödinger (NLS) equation are unstable, with the solitary wave's amplitude becoming infinite in finite time above an amplitude threshold and the amplitude decaying to zero below the threshold [5]. Theoretical work by Conti *et al.* [2] showed that a nematicon is stable due to the nonlocal nature of its interaction with the nematic, whereby the director profile is much wider than the waist of the beam in the light. Moreover, as the nematicon equations are the same as those for a thermoelastic waveguide, the work of Kuznetsov and Rubenchik [6] shows that a nematicon is stable.

While guided wave propagation in nematic liquid crystals is usually considered in the nonlocal limit, adjusting the experimental conditions, such as temperature and applied static electric fields, can result in local interaction between light and the nematic [7], in which case the director profile has a width of the same order as the beam [8,9]. In this local case the nematicon is stable since the nematicon equations reduce to a saturating NLS equation [5,8,9].

The first work on nematicon propagation in nematic liquid crystals considered the propagation of a beam or beams of the same wavelength [1–4,10–12]. Recent work by Alberucci *et al.* [13] studied the propagation and interaction of nematicons of two colors (wavelengths). This work derived the governing equations for the propagation of two beams of different wavelengths through a nematic liquid crystal and then compared numerical solutions of these equations with experimental results. Excellent agreement was obtained.

In the present work the dynamics of interacting two color nematicons in the local limit will be studied using a variational method based on that of García-Reimbert *et al.* [8] for a single nematicon. The main propagation mode in which we shall be interested is that for which the two nematicons form a bound vector nematicon. One of the important advantages of the variational method of García-Riembert *et al.* [8,9] is that it provides a method for the inclusion of the effect of the diffractive radiation shed as a nematicon evolves. The effect of this shed radiation will be included in the modulation equations derived here from the two color nematicon equations in the local limit. The inclusion of this shed diffractive radiation is found to be vital to obtain good agreement with full numerical solutions of the two color nematicon equations. Due to the nonsymmetric optical parameters for the two colors, momentum conservation gives that the vector nematicon experiences walk-off, as found in Alberucci *et al.* [13]. Without the inclusion of diffractive radiation loss the walk-off predicted by the modulation equations differs from the numerical walk-off by up to 30%, while when diffractive radiation loss is included the modulation equations give a walk-off within 1% of the numerical value.

II. APPROXIMATE EQUATIONS

Let us consider two polarized, coherent light beams of two different wavelengths propagating through a cell filled with a nematic liquid crystal, as illustrated in Fig. 1. The light initially propagates in the z direction, with the (x,y) plane orthogonal to this. A static electric field is applied in the x direction so that in the absence of light the optical director is pretilted at an angle $\hat{\theta}$ to the z direction. Both input light beams are polarized with their electric fields in the x direction. Then let u and v be the electric field envelopes of the two light beams and θ be the perturbation of the

*s0096088@sms.ed.ac.uk
†N.Smyth@ed.ac.uk

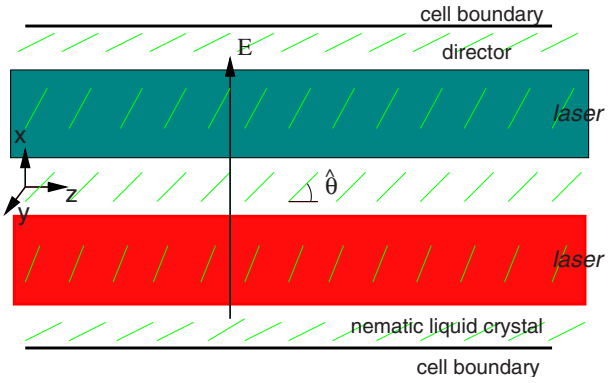

FIG. 1. (Color online) Schematic diagram of a liquid crystal cell with two polarized light beams of different colors.

optical director angle from its static value due to the light beams. The two color nematicon equations governing this were derived in Alberucci *et al.* [13]. In nondimensional form these equations are

$$i\frac{\partial u}{\partial z}+\frac{1}{2}D_u\nabla^2 u+A_u u\sin 2\theta=0, \tag{1}$$

$$i\frac{\partial v}{\partial z}+\frac{1}{2}D_v\nabla^2 v+A_v v\sin 2\theta=0, \tag{2}$$

$$\nu\nabla^2\theta-q\sin 2\theta=-2A_u|u|^2\cos 2\theta-2A_v|v|^2\cos 2\theta. \tag{3}$$

The Laplacian ∇^2 is in the (x,y) plane. The coefficients D_u and D_v are the diffraction coefficients for the two colors and A_u and A_v are the coupling coefficients between the light and the nematic for the two colors. The parameter ν measures the elasticity of the nematic and q is related to the energy of the static electric field which pretilts the nematic [14].

The usual operating regime for beam propagation in nematics has ν large, the so-called nonlocal regime. However, by varying the operating temperature and the strength of the pretilt field (q), ν can be made to take a range of values from small (the local regime) to large (the nonlocal regime) [7]. In the present work two color nematicon evolution will be considered in the local regime with ν small. For small ν the director Eq. (3) reduces to

$$\tan 2\theta=\frac{2}{q}(A_u|u|^2+A_v|v|^2). \tag{4}$$

With this expression for the director angle, the electric field Eqs. (1) and (2) become

$$i\frac{\partial u}{\partial z}+\frac{1}{2}D_u\nabla^2 u+\frac{2A_u(A_u|u|^2+A_v|v|^2)u}{\sqrt{q^2+4(A_u|u|^2+A_v|v|^2)^2}}=0,$$

$$i\frac{\partial v}{\partial z}+\frac{1}{2}D_v\nabla^2 v+\frac{2A_v(A_u|u|^2+A_v|v|^2)v}{\sqrt{q^2+4(A_u|u|^2+A_v|v|^2)^2}}=0. \tag{5}$$

So in the local regime the propagation of the two color nematicons is governed by a system of vector saturating nonlinear Schrödinger equations.

The vector system (5) has the Lagrangian

$$L=i(u^*u_z-uu_z^*)-D_u|\nabla u|^2+i(v^*v_z-vv_z^*)-D_v|\nabla v|^2+\sqrt{q^2+4(A_u|u|^2+A_v|v|^2)^2}-q, \tag{6}$$

where the superscript * denotes the complex conjugate. As in [8,9] approximate solutions will now be sought using appropriate trial functions in the averaged Lagrangian

$$\mathcal{L}=\int_{-\infty}^{\infty}\int_{-\infty}^{\infty}L dxdy. \tag{7}$$

The first trial function to be used in the present work is that of García-Reimbert *et al.* [8,9], so that the trial functions for the electric field envelopes u and v are taken in the form

$$u=a_u\,\mathrm{sech}\frac{\chi_u}{w_u}e^{i\psi_u}+ig_u e^{i\psi_u},$$

$$v=a_v\,\mathrm{sech}\frac{\chi_v}{w_v}e^{i\psi_v}+ig_v e^{i\psi_v}, \tag{8}$$

where

$$\chi_u=\sqrt{(x-\xi_u)^2+y^2},\quad \chi_v=\sqrt{(x-\xi_v)^2+y^2},$$

$$\psi_u=\sigma_u+V_u(x-\xi_u),\quad \psi_v=\sigma_v+V_v(x-\xi_v). \tag{9}$$

The electric field amplitudes a_u, a_v, widths w_u, w_v, nematicon positions ξ_u, ξ_v, velocities V_u, V_v, phases σ_u, σ_v, and shelf heights g_u, g_v are functions of z. The first terms in the trial functions (8) are varying solitary waves. The second terms represent the effect of the shed diffractive radiation of low wave number which accumulates under the evolving nematicons [8,9,15]. This shed radiation cannot remain flat, so it is assumed that g_u (g_v) is nonzero in the disk $0\le\sqrt{(x-\xi_u)^2+y^2}\le R_u$ $(0\le\sqrt{(x-\xi_v)^2+y^2}\le R_v)$ [8,9,15]. In the case of the $1+1$ dimensional NLS equation the existence of this shelf of low wave-number radiation under the pulse can be shown using inverse scattering [15].

The trial functions (8) are now substituted into the averaged Lagrangian (7), from which variational equations are obtained for the nematicon parameters. However, the integrals involving the nonlinear term (last term) in the Lagrangian (6) cannot be evaluated in closed form. To overcome this, it is assumed, as in García-Reimbert *et al.* [8], that the amplitudes of the two nematicons are small (or that q is large), so that the square root can be expanded in a Taylor series. While this then allows most of the integrals to be evaluated, a few integrals involving products of u and v still cannot be evaluated. To evaluate these cross integrals, such as

$$\int_{-\infty}^{\infty}\int_{-\infty}^{\infty}|u|^2|v|^2dxdy, \tag{10}$$

the idea of an "equivalent" Gaussian is used [9,16]. For these cross integrals only the trial functions are replaced by the "equivalent" Gaussians,

$$\operatorname{sech}\frac{\chi_u}{w_u} \to \alpha e^{-\chi_u^2/(\beta^2 w_u^2)}, \quad \operatorname{sech}\frac{\chi_v}{w_v} \to \alpha e^{-\chi_v^2/(\beta^2 w_v^2)}, \quad (11)$$

so that these cross integrals can be evaluated in closed form. The scaling parameters α and β will be determined by matching the resulting averaged Lagrangian with the known averaged Lagrangian in the symmetric limit $A_u=A_v$ and $D_u=D_v$ with $\xi_u=\xi_v$, for which the averaged Lagrangian is that of García-Reimbert *et al.* [8]. Later in this section, Gaussian trail functions will also be considered, for which this "equivalent" Gaussian substitution is obviously not needed.

Using this small amplitude expansion and the "equivalent" Gaussian the averaged Lagrangian (7) is

$$\begin{aligned}\mathcal{L} = &-2(I_2 a_u^2 w_u^2 + \Lambda_u g_u^2)(\sigma_u' - V_u \xi_u') - 2I_1 a_u w_u^2 g_u' + 2I_1 w_u^2 g_u a_u' \\ &+ 4I_1 a_u w_u g_u w_u' - ID_u a_u^2 - D_u(I_2 a_u^2 w_u^2 + \Lambda_u g_u^2)V_u^2 \\ &-2(I_2 a_v^2 w_v^2 + \Lambda_v g_v^2)(\sigma_v' - V_v \xi_v') - 2I_1 a_v w_v^2 g_v' + 2I_1 w_v^2 g_v a_v' \\ &+ 4I_1 a_v w_v g_v w_v' - ID_v a_v^2 - D_v(I_2 a_v^2 w_v^2 + \Lambda_v g_v^2)V_v^2 \\ &+ \frac{2}{q}Q_1 - \frac{2}{q^3}Q_2, \end{aligned} \quad (12)$$

where

$$\begin{aligned}Q_1 = &A_u^2 I_4 a_u^4 w_u^2 + A_v^2 I_4 a_v^4 w_v^2 \\ &+ \frac{1}{2}\frac{A_u A_v}{S_1}\alpha^4 \beta^2 a_u^2 a_v^2 w_u^2 w_v^2 e^{-2(\xi_u - \xi_v)^2/(\beta^2 S_1)}, \end{aligned}$$

$$\begin{aligned}Q_2 = &A_u^4 I_8 a_u^8 w_u^2 + A_v^4 I_8 a_v^8 w_v^2 \\ &+ \frac{A_u^3 A_v}{S_2}\alpha^8 \beta^2 a_u^6 a_v^2 w_u^2 w_v^2 e^{-6(\xi_u - \xi_v)^2/(\beta^2 S_2)} \\ &+ \frac{3}{4}\frac{A_u^2 A_v^2}{S_1}\alpha^8 \beta^2 a_u^4 a_v^4 w_u^2 w_v^2 e^{-4(\xi_u - \xi_v)^2/(\beta^2 S_1)} \\ &+ \frac{A_u A_v^3}{S_3}\alpha^8 \beta^2 a_u^2 a_v^6 w_u^2 w_v^2 e^{-6(\xi_u - \xi_v)^2/(\beta^2 S_3)} \end{aligned} \quad (13)$$

with

$$S_1 = w_u^2 + w_v^2, \quad S_2 = w_u^2 + 3w_v^2, \quad S_3 = 3w_u^2 + w_v^2. \quad (14)$$

Also Λ_u and Λ_v are related to the shelf radii by

$$\Lambda_u = \frac{1}{2}R_u^2 \text{ and } \Lambda_v = \frac{1}{2}R_v^2. \quad (15)$$

The nonlinear terms Q_1 and Q_2 result from the expansion of the nonlinear term in the Lagrangian (6). The various integrals I and I_i resulting from the calculation of this averaged Lagrangian are

$$I = \int_0^\infty x \operatorname{sech}^2 x \tanh^2 x \, dx = \frac{1}{3}\ln 2 + \frac{1}{6},$$

$$I_1 = \int_0^\infty x \operatorname{sech} x \, dx = 2C,$$

$$I_2 = \int_0^\infty x \operatorname{sech}^2 x \, dx = \ln 2,$$

$$I_4 = \int_0^\infty x \operatorname{sech}^4 x \, dx = \frac{2}{3}\ln 2 - \frac{1}{6},$$

$$I_8 = \int_0^\infty x \operatorname{sech}^8 x \, dx = \frac{16}{35}\ln 2 - \frac{19}{105}, \quad (16)$$

where C is the Catalan constant $C=0.915\,965\,594\ldots$ [17].

The scaling parameters α and β for the "equivalent" Gaussian (11) can now be determined by matching the averaged Lagrangian (12) with the averaged Lagrangian of García-Reimbert *et al.* [8] in the symmetric limit $A_u=A_v$, $D_u=D_v$, $a_u=a_v$, $w_u=w_v$, $g_u=g_v$, $V_u=V_v=0$, $\xi_u=\xi_v$, $\sigma_u=\sigma_v$. This gives

$$\alpha^4 = \frac{2I_8}{I_4} \text{ and } \beta^2 = \frac{4I_4^2}{I_8}. \quad (17)$$

The scaling parameters are then $\alpha=0.9794\ldots$ and $\beta=1.6027\ldots$, so that the "equivalent" Gaussian has nearly the same amplitude as the original trial function with the major change being a different width.

Taking variations of the averaged Lagrangian (12) with respect to the nematicon parameters, and after some algebra, finally results in the modulation equations

$$\frac{d}{dz}(I_2 a_u^2 w_u^2 + \Lambda_u g_u^2) = 0, \quad (18)$$

$$\frac{d}{dz}(I_1 a_u w_u^2) = \Lambda_u g_u\left(\sigma_u' - V_u \xi_u' + \frac{1}{2}D_u V_u^2\right), \quad (19)$$

$$\begin{aligned}I_1 \frac{dg_u}{dz} = &\frac{1}{2}D_u a_u w_u^{-2} - \frac{1}{2qa_u w_u^2}\left(a_u \frac{\partial Q_1}{\partial a_u} - w_u \frac{\partial Q_1}{\partial w_u}\right) \\ &+ \frac{1}{2q^3 a_u w_u^2}\left(a_u \frac{\partial Q_2}{\partial a_u} - w_u \frac{\partial Q_2}{\partial w_u}\right), \end{aligned} \quad (20)$$

$$\begin{aligned}I_2\left(\frac{d\sigma_u}{dz} - V_u \frac{d\xi_u}{dz}\right) = &-ID_u w_u^{-2} - \frac{1}{2}D_u I_2 V_u^2 \\ &+ \frac{1}{2qa_u^2 w_u^2}\left(2a_u \frac{\partial Q_1}{\partial a_u} - w_u \frac{\partial Q_1}{\partial w_u}\right) \\ &- \frac{1}{2q^3 a_u^2 w_u^2}\left(2a_u \frac{\partial Q_2}{\partial a_u} - w_u \frac{\partial Q_2}{\partial w_u}\right), \end{aligned} \quad (21)$$

$$\frac{d}{dz}[(I_2 a_u^2 w_u^2 + \Lambda_u g_u^2)V_u] = \frac{1}{q}\frac{\partial Q_1}{\partial \xi_u} - \frac{1}{q^3}\frac{\partial Q_2}{\partial \xi_u}, \quad (22)$$

$$\frac{d\xi_u}{dz} = D_u V_u, \quad (23)$$

plus symmetric equations for a_v, w_v, σ_v, g_v, V_v, and ξ_v. The modulation Eq. (18) is the equation for conservation of mass

and Eq. (22), when added to the symmetric equation in the v color, is the equation for the conservation of momentum, in the sense of invariances of the Lagrangian (6) [18]. However, in the current context of optics, these conserved quantities do not physically correspond to mass and momentum. For instance, the conserved quantity of Eq. (18) is actually the optical power.

Nöther's theorem applied to the Lagrangian (6) shows that the local nematicon Eqs. (5) possess the energy conservation equation

$$\frac{dH}{dz} = \int_{-\infty}^{\infty}\int_{-\infty}^{\infty} [D_u|\nabla u|^2 + D_v|\nabla v|^2 - \sqrt{q^2 + 4(A_u|u|^2 + A_v|v|^2)^2} + q]dxdy = 0. \quad (24)$$

Using the trial functions (8) then gives the energy conservation equation for the two color nematicons,

$$\frac{dH}{dz} = \frac{d}{dz}\left[ID_u a_u^2 + ID_v a_v^2 - \frac{2}{q}Q_1 + \frac{2}{q^3}Q_2 \right] = 0, \quad (25)$$

on using the mass and momentum Eqs. (18) and (22) and their v color counterparts.

The final quantities to determine are the shelf radii R_u and R_v. In previous work involving the NLS equation [15] and the single color nematicon equations [8,9,16], the shelf radius was determined by linearizing the modulation equations about their fixed point, which resulted in a simple harmonic oscillator equation. The frequency of this oscillator equation, which depends on the shelf width, was then matched to the soliton oscillation frequency, resulting in an expression for the shelf width. The same analysis could be performed for the present modulation equations. However, this results in complicated expressions for R_u and R_v. Much simplified expressions for the shelf radii can be obtained on noting that in dimensional variables the diffraction coefficients and the coupling coefficients for the two colors have similar values. For instance, for the experiments of Alberucci *et al.* [13] the diffraction coefficients were 0.805 for red light and 0.823 for near-infrared light. It is then reasonable to take values of D_u, D_v and A_u, A_v which are close to each other. In the symmetric limit $D_u = D_v$ and $A_u = A_v$, the local nematicon Eqs. (5) become a coupled pair of the local nematicon equation considered by García-Reimbert *et al.* [8]. On rescaling their shelf radius, as García-Reimbert *et al.* [8] had $D_u = 1$ and $A_u = 1$, we have

$$\Lambda_u = \frac{II_1^2 D_u q^3}{384 I_2 I_8 A_u^4 \hat{a}_u^6} \quad \text{and} \quad \Lambda_v = \frac{II_1^2 D_v q^3}{384 I_2 I_8 A_v^4 \hat{a}_v^6}. \quad (26)$$

From García-Reimbert *et al.* [8] the fixed point amplitudes $\hat{a}_u$ and $\hat{a}_v$ are given by

$$\hat{a}_u^6 = -\frac{I_4 q^2 H}{16 I I_8 D_u A_u^2} \quad \text{and} \quad \hat{a}_v^6 = -\frac{I_4 q^2 H}{16 I I_8 D_v A_v^2}, \quad (27)$$

where H is the energy given by Eq. (25). In these expressions to determine the shelf radii the appropriate values of the diffraction and coupling coefficients for the two colors have been used to preserve symmetry.

The trial functions (8) were assumed to have the same sech profile as the soliton solution of the NLS equation. Another possible choice for the trial functions is a Gaussian, particularly as this choice obviates the need for an "equivalent" function in order to explicitly calculate various cross integrals in the averaged Lagrangian. In this regard it was shown by Conti *et al.* [2] that a nematicon has a Gaussian profile near its peak and that its tail decays as the modified Bessel function of order zero K_0, due to the circular symmetry. A Gaussian trial function then gives a better representation of the nematicon near its peak, while the sech profile gives a better representation of its decay away from its peak. To further understand the effect of the choice of trial function, modulation equations will also be derived for the Gaussian trial functions,

$$u = a_u e^{-(\chi_u/w_u)^2} e^{i\psi_u} + i g_u e^{i\psi_u},$$

$$v = a_v e^{-(\chi_v/w_v)^2} e^{i\psi_v} + i g_v e^{i\psi_v}. \quad (28)$$

No new calculations are required for these new trial functions. All that is required is to replace the integrals (16) by

$$I = \int_0^{\infty} x(-2xe^{-x^2})^2 dx = \frac{1}{2},$$

$$I_1 = \int_0^{\infty} xe^{-x^2} dx = \frac{1}{2},$$

$$I_2 = \int_0^{\infty} xe^{-2x^2} dx = \frac{1}{4},$$

$$I_4 = \int_0^{\infty} xe^{-4x^2} dx = \frac{1}{8},$$

$$I_8 = \int_0^{\infty} xe^{-8x^2} dx = \frac{1}{16}. \quad (29)$$

The averaged Lagrangian is then Eq. (12) and the modulation equations are Eqs. (18)–(23) with these replacements for the integrals I and I_i. Obviously in this Gaussian case $\alpha = 1.0$ and $\beta = 1.0$, which can also be derived from Eqs. (17) and (29). It should be noted that the averaged Lagrangian (12) and the modulation Eqs. (18)–(23) hold for any self-similar trial function for u and v. All that is needed is that the integrals I and I_i of Eq. (16) are replaced by the equivalent first moments of powers of this trial function and its first derivative.

Much information about the evolution of the two color nematicons can be obtained by looking at the fixed point of the modulation Eqs. (18)–(23). These modulation equations possess two types of fixed points: (i) a coupled vector nematicon with $\xi_u = \xi_v$, and (ii) separate nematicons, which become the one color nematicons of García-Reimbert *et al.* [8] as $|\xi_u - \xi_v| \to \infty$. In the present work we shall be interested in the vector nematicon propagation mode. Let us denote fixed point values of the nematicon parameters by $\hat{}$ and boundary

values at $z=0$ by a 0 subscript. Adding the momentum Eq. (22) in the u color to its symmetric counterpart in the v color gives the equation for total momentum conservation as

$$\frac{d}{dz}[(I_2a_u^2w_u^2+\Lambda_u g_u^2)V_u+(I_2a_v^2w_v^2+\Lambda_v g_v^2)V_v]=0. \quad (30)$$

As we are considering boundary conditions which lead to a bound state of the two colors, $\hat{\xi}_u=\hat{\xi}_v$ for these boundary conditions. On noting that $g_{u0}=g_{v0}=0$ and $\hat{g}_u=\hat{g}_v=0$, the mass and momentum conservation Eqs. (18) and (30), plus the position relation (23), therefore give

$$\hat{\xi}_u'=\hat{\xi}_v'=\frac{D_uD_vM_0}{I_2(D_va_{u0}^2w_{u0}^2+D_ua_{v0}^2w_{v0}^2)}, \quad (31)$$

where

$$M_0=I_2a_{u0}^2w_{u0}^2V_{u0}+I_2a_{v0}^2w_{v0}^2V_{v0} \quad (32)$$

is the total initial momentum. The conservation expression (31) then gives the walk-off of the vector nematicon in the two colors.

III. DIFFRACTIVE RADIATION LOSS

To complete the modulation Eqs. (18)–(23), the effect of the diffractive radiation shed by the nematicons as they evolve must be included. Numerical solutions show that the shed radiation has small amplitude relative to the nematicons. Hence this radiation is governed by the Schrödinger equations

$$i\frac{\partial u}{\partial z}+\frac{1}{2r}D_u\frac{\partial}{\partial r}\left(r\frac{\partial u}{\partial r}\right)=0,$$

$$i\frac{\partial v}{\partial z}+\frac{1}{2r}D_v\frac{\partial}{\partial r}\left(r\frac{\partial v}{\partial r}\right)=0. \quad (33)$$

This radiation problem has already been studied by García-Reimbert *et al.* [8] and so the details will not be repeated. The final result is that the mass Eq. (18) and Eq. (20) for the radiation shelf height g_u are replaced by

$$\frac{d}{dz}(I_2a_u^2w_u^2+\Lambda_u g_u^2)=-2D_u\delta_u\Lambda_uR_u^2 \quad (34)$$

and

$$I_1\frac{dg_u}{dz}=\frac{1}{2}D_ua_uw_u^{-2}-\frac{1}{2qa_uw_u^2}\left(a_u\frac{\partial Q_1}{\partial a_u}-w_u\frac{\partial Q_1}{\partial w_u}\right)+\frac{1}{2q^3a_uw_u^2}\left(a_u\frac{\partial Q_2}{\partial a_u}-w_u\frac{\partial Q_2}{\partial w_u}\right)-2D_u\delta_ug_u, \quad (35)$$

respectively, where the loss coefficient δ_u is

$$\delta_u=-\frac{\sqrt{2\pi}I_1}{2eR_u\Lambda_u}\int_0^z\pi R_u(z')\ln[(z-z')/\Lambda_u]\left\{\left[\left(\frac{1}{2}\ln[(z-z')/\Lambda_u]\right)^2+\frac{3\pi^2}{4}\right]^2+\pi^2\{\ln[(z-z')/\Lambda_u]\}^2\right\}^{-1}\frac{dz'}{(z-z')} \quad (36)$$

and

$$R_u^2=\frac{1}{\Lambda_u}[I_2a_u^2w_u^2-I_2\hat{a}_u^2\hat{w}_u^2+\Lambda_ug_u^2]. \quad (37)$$

The variable R_u measures the difference between the mass of the u color at z and its mass at the fixed point. The mass equation for the v color and the equation for g_v are obtained by the obvious symmetric substitutions.

With the inclusion of the diffractive radiation loss, the modulation equations for the two color nematicons are complete.

IV. RESULTS AND COMPARISONS WITH NUMERICAL SOLUTIONS

In this section solutions of the modulation Eqs. (19), (21)–(23), (34), and (35) and their symmetric v counterparts will be compared with full numerical solutions of the two color nematicon Eqs. (1)–(3). The modulation equations were solved using the standard fourth order Runge-Kutta scheme. The electric field Eqs. (1) and (2) were solved using a pseudospectral method based on that of Fornberg and Whitham [19]. The main difference with the scheme of Fornberg and Whitham is that the stepping in the z direction was performed in Fourier space using a fourth order Runge-Kutta method, rather than in physical space using a second order scheme. The director Eq. (3) was rewritten in the form

$$\nu\nabla^2\theta-2q\theta=q\sin(2\theta)-2q\theta-2A_u|u|^2\cos(2\theta)-2A_v|v|^2\cos(2\theta). \quad (38)$$

On taking fast Fourier transforms (FFT's) in the x direction, the resulting nonlinear two point boundary value problem in y, with θ vanishing at the edges of the computational domain, was solved using a Picard iteration with the Fourier transform of the right hand side of Eq. (38) evaluated at the previous iteration. The director equation was rewritten in the form (38) as this form was found to have better convergence properties.

Figure 2 shows a comparison of the values of the walk-off $\hat{\xi}'=\hat{\xi}_u'=\hat{\xi}_v'$ as given by the full numerical solution of the two color nematicon Eqs. (1)–(3), the solution of the modulation equations, and the momentum conservation result (31) as a function of V_{v0} for sech initial conditions (8) which result in the formation of a vector nematicon, where V_{v0} is the initial value of V_v. The numerical and modulation solutions do not settle to the steady state until large values of z are reached. This slow evolution to the steady state is typical of nematicon evolution [8,9,16]. To enable a large number of numerical runs to be made in a reasonable time, the numerical solutions were run until the oscillations of the positions of the

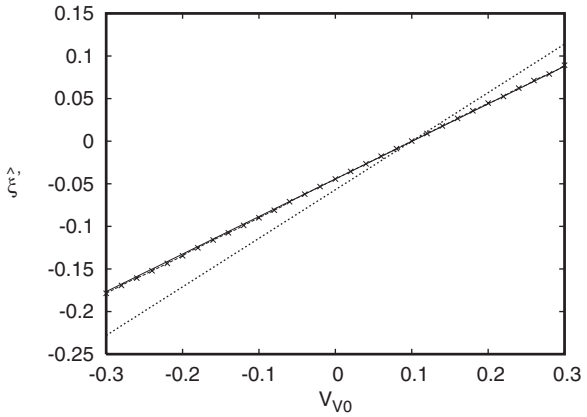

FIG. 2. Steady value $\hat{\xi}'=\hat{\xi}_u'=\hat{\xi}_v'$ as a function of V_{v0} for the initial conditions $a_u=0.35$, $a_v=0.35$, $w_u=3.0$, $w_v=3.0$, $V_u=-0.1$, $\xi_u=1.0$, and $\xi_v=-1.0$ with $D_u=1.0$, $D_v=0.8$, $A_u=1.0$, and $A_v=0.9$ for the sech initial condition (8). Full numerical solution (—), solution of modulation Eqs. (19), (21)–(23), (34), and (35) (– × – × –), momentum conservation result (31) (- - -).

nematicons about the final state were small and then an average was taken of these oscillations to determine $\hat{\xi}'$. It can be seen that there is near perfect agreement between the numerical and modulation solutions for the walk-off. The momentum conservation result (31) was derived on the assumption that the nematicons do not shed mass and momentum. It is therefore apparent that the inclusion of the mass and momentum shed by the nematicons as they evolve is vital in order to obtain good agreement with numerical solutions.

Figure 3 shows a similar comparison to Fig. 2 for the walk-off, except that the Gaussian profile (28) was used as the initial condition. The results are similar to those for the sech profile, with near perfect agreement between the numerical and modulation solutions. Again the inclusion of shed mass and momentum is vital in order to obtain good agreement with full numerical solutions. Inspection of Figs. 2 and 3 shows that there is little difference in the agreement

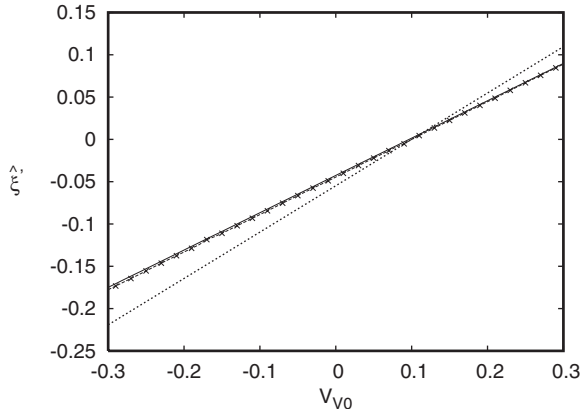

FIG. 3. Steady value $\hat{\xi}'=\hat{\xi}_u'=\hat{\xi}_v'$ as a function of V_{v0} for the initial conditions $a_u=0.35$, $a_v=0.35$, $w_u=5.0$, $w_v=5.0$, $V_u=-0.1$, $\xi_u=1.0$, and $\xi_v=-1.0$ with $D_u=1.0$, $D_v=0.8$, $A_u=1.0$, and $A_v=0.9$ for the Gaussian initial condition (28). Full numerical solution (—), solution of modulation Eqs. (19), (21)–(23), (34), and (35) (– × – × –); momentum conservation result (31) (- - -).

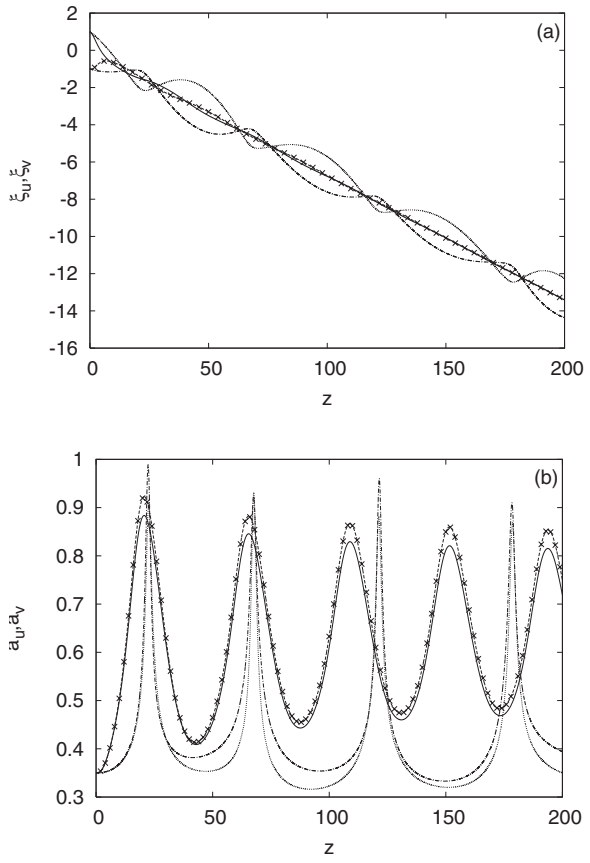

FIG. 4. Solution of two color nematicon equations for the sech profile (8) for the initial conditions $a_u=0.35$, $a_v=0.35$, $w_u=3.0$, $w_v=3.0$, $V_u=-0.1$, $V_v=-0.05$, $\xi_u=1.0$, and $\xi_v=-1.0$ with $D_u=1.0$, $D_v=0.8$, $A_u=1.0$, and $A_v=0.9$. Full numerical solution for u (—), full numerical solution for v (– × – × –), solution of modulation Eqs. (19), (21)–(23), (34), and (35) for u (- - -) and v (– – –). (a) Positions ξ_u, ξ_v, (b) amplitudes a_u, a_v.

with full numerical solutions between the results for the sech and the Gaussian trial functions. From the discussion of the use of a Gaussian trial function in Sec. II this may have been expected as the sech and Gaussian profiles are good approximations to the actual nematicon solution in different regions. The vital point with the use of various trial functions is that as long as the equations for certain basic gross quantities, such as mass, momentum, and energy, are satisfied, then enough constraints are placed on the approximate equations to give good agreement with numerical solutions.

Let us now compare the numerical and modulation results for the evolution of the nematicons. Figure 4 shows a comparison between the full numerical and modulation solutions for the sech trial function (8) for one of the cases leading to a vector nematicon shown in Fig. 2. Figure 4(a) shows the positions ξ_u and ξ_v and Fig. 4(b) shows the amplitudes a_u and a_v as functions of z. As expected from Fig. 2 the agreement for the positions of the two nematicons is excellent in the mean (walk-off). However, the oscillation amplitude of the modulation solution about this mean is greater than the numerical amplitude. Before discussing the reasons for this, let

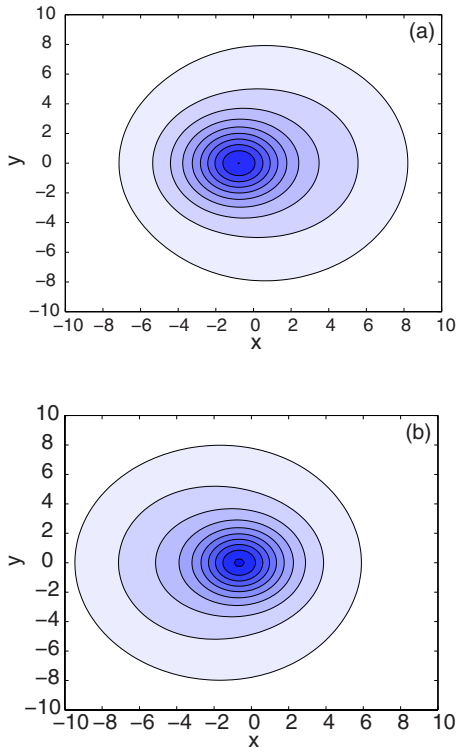

FIG. 5. (Color online) Numerical solution of two color nematicon equations for the sech profile (8) for the initial conditions $a_u=0.35$, $a_v=0.35$, $w_u=3.0$, $w_v=3.0$, $V_u=-0.1$, $V_v=-0.05$, $\xi_u=1.0$, and $\xi_v=-1.0$ with $D_u=1.0$, $D_v=0.8$, $A_u=1.0$, and $A_v=0.9$. (a) Contour plot of numerical solution for $|u|$ at $z=10$, (b) contour plot of numerical solution for $|v|$ at $z=10$.

us look at the amplitude comparison. As for the position comparison, the means of the amplitude oscillations are in good agreement. However, the peak amplitudes as given by the modulation equations are about 7% higher than the numerical peak amplitudes. As the evolution of the nematicons is a nonlinear oscillator, this amplitude difference means that there is also a period difference in the oscillations, which accounts for the increasing difference in the peak amplitude positions of the numerical and modulation solutions.

There are a number of reasons for these differences between the numerical and approximate solutions. The first can be seen from the numerical solutions for $|u|$ and $|v|$ at $z=10$ shown in Figs. 5(a) and 5(b). These solutions are at a value of z just after the point at which the two colors first cross position. It can be seen that the two nematicons have become distorted by their collision. This distortion is, of course, not accounted for in the variational approximation since the symmetric shapes of the two nematicons are fixed by the trial functions (8). This distortion will make a difference to the subsequent evolution of the nematicons. In particular, Fig. 4(a) shows that it results in a rapid decrease in the amplitude of oscillation of the nematicon positions about the mean. Furthermore, as discussed in Smyth and Kath [20], the radiation calculation of Sec. III does not take into account the acceleration of the nematicons. The inclusion of acceleration effects in the mass and momentum loss is a difficult calculation as it involves the solution of a moving boundary value problem with an unknown boundary [20]. Similar amplitude and position comparisons are not shown for the Gaussian trial function as there is little difference in the comparison with numerical solutions, as for the walk-off comparisons of Figs. 2 and 3.

As the initial velocity difference between the nematicons increases, the nematicons become more distorted due to their interaction. This results in the difference in the amplitudes of the position oscillations about the mean (walk-off) as given by the numerical and modulation solutions becoming greater. Also for large velocity differences, the approximate amplitude oscillations gain a second frequency due an interaction with the large position oscillations which oscillate at a different frequency. The numerical solution does not have this second frequency as the distortion of the nematicons due to their interaction results in a rapid damping of their position oscillations about the mean walk-off. However, this increasing difference for the oscillations does not change the excellent agreement for the walk-off, as shown in Figs. 2 and 3. In the limit of large velocity differences, it was found that the Gaussian trial function (28) gave somewhat better agreement for the amplitude evolution, while there was little difference between the Gaussian and sech trial functions for the position evolution.

V. CONCLUSIONS

The interaction of two solitary waves (nematicons) of two different wavelengths (colors) in a nematic liquid crystal in the local limit has been studied using a variational approximation using two different trial functions, a sech and a Gaussian. The variational equations derived were augmented to include the effect of the diffractive radiation shed as the nematicons evolve. Initial conditions for which the two nematicons form a vector nematicon were considered. It was found that the modulation equations gave near perfect agreement with numerical solutions for the walk-off of the steady vector nematicon. The inclusion of the effect of the shed diffractive radiation was vital for this agreement, as it was shown that there is up to a 30% difference in the walk-off if radiation loss is not included, while there is 1% difference or less if it is.

As the nematicons in the two colors interact they become distorted, this distortion increasing as their initial velocity difference increases. As the distortion of the nematicons increases, they shed more radiation so that they can revert to a symmetric profile. As the trial functions did not include modes to account for distortion, increasing differences in the oscillatory components of the nematicons' evolution were found. However, these increasing differences did not affect the excellent agreement for the walk-off. The inclusion of more modes and parameters to account for this distortion in the trial functions is nontrivial as the distortion modes are unknown. Furthermore, the inclusion of more parameters in the trial function results in more complicated modulation equations, which makes it increasingly difficult to obtain

qualitative information from them and negates the point of using simple trial functions to obtain the key features of the evolution.

The extensions of the present work to two color nematicon evolution in a nematic liquid crystal in the nonlocal limit and to the interaction of two color nematicons with angular momentum are currently under investigation.

ACKNOWLEDGMENTS

The authors would like to thank Alessandro Alberucci of the University of Rome III for helpful discussions related to this work. This research was supported by the Engineering and Physical Sciences Research Council (EPSRC-GB) under Grant No. EP/C548612/1.

[1] G. Assanto, M. Peccianti, and C. Conti, Opt. Photonics News **14**, 45 (2003).
[2] C. Conti, M. Peccianti, and G. Assanto, Phys. Rev. Lett. **91**, 073901 (2003).
[3] G. Assanto and M. Peccianti, IEEE J. Quantum Electron. **39**, 13 (2003).
[4] C. Conti, M. Peccianti, and G. Assanto, Phys. Rev. Lett. **92**, 113902 (2004).
[5] Y. S. Kivshar and G. P. Agrawal, *Optical Solitons. From Fibers to Photonic Crystals* (Academic Press, San Diego, 2003).
[6] E. A. Kuznetsov and A. M. Rubenchik, Phys. Rep. **142**, 103 (1986).
[7] A. Fratalocchi and G. Assanto, Phys. Rev. E **72**, 066608 (2005).
[8] C. García Reimbert, A. A. Minzoni, and N. F. Smyth, J. Opt. Soc. Am. B **23**, 294 (2006).
[9] C. García-Reimbert, A. A. Minzoni, N. F. Smyth, and A. L. Worthy, J. Opt. Soc. Am. B **23**, 2551 (2006).
[10] M. Peccianti, K. A. Brzdiąkiewicz, and G. Assanto, Opt. Lett. **27**, 1460 (2002).
[11] G. Assanto, M. Peccianti, K. A. Brzdiąkiewicz, A. de Luca, and C. Umeton, J. Nonlinear Opt. Phys. Mater. **12**, 123 (2003).
[12] A. Fratalocchi, M. Peccianti, C. Conti, and G. Assanto, Mol. Cryst. Liq. Cryst. **421**, 197 (2004).
[13] A. Alberucci, M. Peccianti, G. Assanto, A. Dyadyusha, and M. Kaczmarek, Phys. Rev. Lett. **97**, 153903 (2006).
[14] C. García Reimbert, C. Garza Hume, A. A. Minzoni, and N. F. Smyth, Physica D **167**, 136 (2002).
[15] W. L. Kath and N. F. Smyth, Phys. Rev. E **51**, 1484 (1995).
[16] A. A. Minzoni, N. F. Smyth, and A. L. Worthy, J. Opt. Soc. Am. B **24**, 1549 (2007).
[17] M. Abramowitz and I. A. Stegun, *Handbook of Mathematical Functions with Formulas, Graphs and Mathematical Tables* (Dover Publications, Inc., New York, 1972).
[18] D. J. Kaup and A. C. Newell, Proc. R. Soc. London, Ser. A **361**, 413 (1978).
[19] B. Fornberg and G. B. Whitham, Philos. Trans. R. Soc. London, Ser. A **289**, 373 (1978).
[20] N. F. Smyth and W. L. Kath, Phys. Rev. E **63**, 036614 (2001).